Effect of correlations between absorbed and emitted frequencies on the transport of resonance radiation*

M. G. Payne, J. E. Talmage,† G. S. Hurst, and E. B. Wagner

Health Physics Division, Oak Ridge National Laboratory, Oak Ridge, Tennessee 37830

(Received 13 July 1973)

An equation for the transport of resonance radiation at low and intermediate pressures is derived and shown to be in reasonable agreement with an experiment conducted in parallel with the theoretical development. Both dealt with the transport of 1048-Å resonance photons in argon in the pressure range 0.002–10 Torr. At pressures greater than 1 Torr where collisions are frequent, the present transport equation is equivalent to that of Holstein and Biberman. In the pressure region from 0.002 to 0.5 Torr there is substantial disagreement (as much as a factor of 3) between the present work and theory that assumes complete redistribution of frequency, i.e., takes the emission profile to be equal to the absorption profile.

I. INTRODUCTION

After a monatomic gas is excited, photons are soon emitted as a result of transitions between excited states and the ground state. Such light is emitted with a frequency profile centered about some value ν_0 and has a width determined by pressure, atomic species present, atomic level, and temperature. Absorption of the photons is strongest at ν_0 with the absorption profile dropping sharply as $|\nu - \nu_0|$ is increased. In monatomic gases, photons with frequencies very near ν_0 are absorbed so strongly that hundreds or even thousands of absorptions[1-4] and reemissions may occur at typical temperatures and pressures before the energy is either converted to another form or escapes to the container wall. For many years[1,2] such photons, i.e., ones emitted in transitions between excited states and the ground state, have been called "resonance radiation."

Holstein[5] and Biberman[6] treated the transport of resonance radiation on the assumption that there is no correlation between the frequency of an absorbed photon and that of the photon emitted subsequently. Holstein[5] gave rather convincing arguments that this approximation leads to the correct final results in two situations: (i) The result was shown to be correct if the decay of the autocorrelation function $\langle \vec{\mu}(\tau) \cdot \vec{\mu}(t+\tau) \rangle$ is almost complete within a natural lifetime, i.e., $\gamma_c/\gamma \gg 1$. (ii) The result of a transport theory which employs such an approximation was claimed to be approximately correct, at least at late times, even when the pressure is so low that collisions almost never occur within a natural lifetime, and the wings of the Voigt absorption profile produce little effect. In the latter situation, however, it is necessary that the container dimensions be large enough so that strong imprisonment of the resonance radiation occurs, and yet if these dimensions are too large, the "wings" on the absorption profile become important. The work of Holstein predicted the very-late-time behavior for the cases of infinite slab and infinitely long cylindrical geometries. In addition, it concentrated on the limiting cases of pure-Doppler and pure pressure-broadened absorption profiles. Later workers[7] have employed the Holstein-Biberman transport equation in order to extend the theory so that arbitrary initial conditions can be used in predicting $N(\vec{r}, t)$, the number of excited atoms per unit volume at any time t. As in the older work,[5,6] the concentration has been on the limiting cases of pure Doppler and pressure-broadened absorption profiles. It should also be mentioned that a recent Monte Carlo calculation[8] shows that in Holstein's second situation (very low pressures where no collisions occur and the wings of the absorption profile play no part), the results of the Holstein theory become valid within a few natural lifetimes. However, there are very large deviations from the theory at times less than a few natural lifetimes if the gas is excited in a way that leads to many of the first emitted photons being on the far wings of the absorption profile. Many such photons are reemitted on the far wings and escape the container after one or two emissions.

The combined experimental and theoretical study, which is partially reported here, was stimulated by the important role played by resonance trapping in determining the fate of energy deposited by energetic charged particles in the inert gases. Detailed models have been suggested to describe energy pathways in helium and argon excited by fast electrons and protons. These models, due to Bartell, Hurst, and Wagner[9] for

helium and Thonnard and Hurst[10] for argon, are being subjected to detailed checks concerning predictions of time behavior of all radiation that escapes from the system and concerning the balance of energy among the various components of the emerging radiation.

An outline of the remainder of the present paper follows.

Section II. In this section we derive a transport equation that may represent with good accuracy the transport of resonance radiation in a wide range of laboratory situations if it is combined with the results of a line-broadening theory that is valid sufficiently far out on the line wings.

Section III. Very low pressures are studied and it is shown that the Holstein-Biberman equation with a pure Doppler-broadened absorption profile begins to give approximately the same results as the present transport theory within a few natural lifetimes. Thus, we demonstrate the results of Klots and Anderson[8] analytically and establish the time scale involved before complete redistribution in frequency (even though not present in individual absorption and reemission events) becomes almost correct when averaged over several absorptions and reemissions or over space. All that is needed is strong imprisonment of the photons.

Section IV. We investigate the properties of the frequency redistribution function[11,12] and point out what we believe to be the most accurate form presently available. The discussion of how collisions (either frequent or very infrequent) enter into the frequency redistribution function hinges heavily on previous work by Huber[13] and Zanstra.[14] It is shown that for short natural lifetime τ (i.e., $\gamma = \tau^{-1} \gtrsim 10^9/\text{sec}$), large deviations from a theory which employs the Holstein-Biberman equation should occur. This occurs when $P_c \lesssim 0.7$ (where P_c is the probability of at least one decorrelating collision before emission), but at the same time a sizeable fraction of the escaping photons are far enough out on the wings of the absorption profile for the Lorentzian tail to be important. These conditions exist only for short natural lifetime atomic states.

Section V. We discuss a method for examining the early-time escape (early enough so that most of the energy remains in the system) of the photons from the center of an infinite slab of thickness y_0. It is shown (except for a range of pressure that can be determined from theory) that an approximation due to Jefferies and White[15] can be used on the most complicated part of the redistribution function and the resulting equation can be solved analytically with good accuracy.

Section VI. It is pointed out that the 1048-Å

line of argon ($\tau \cong 2.15 \times 10^{-9}$ sec[16]) is well suited for observing deviations from what would be obtained by applying the Holstein-Biberman equation with emission profile $P(x) = k(x)/\pi^{1/2}k(0)$, where $k(x)$ is the Voigt profile version of the absorption coefficient which arises from combining natural and pressure broadening with Doppler broadening.

An experiment is reported which has the following features.

(a) High-purity (99.999%) argon is contained in a long cylinder of radius $R \simeq 1.1$ cm.

(b) The gas is excited by bursts of protons of energy 2.0 MeV and a pulse duration of 17-nsec full width at half-maximum (FWHM). Time between pulses is long enough so that almost all excited atoms produced in one pulse have decayed before the next pulse is incident.

(c) Light from a slablike region (centered on the axis of the cylinder and having dimension y_0 perpendicular to the cylinder's axis) can be seen by the grating of a spectrometer set so that photons with wavelength λ near 1048 Å are detected by a channeltron. Protons are time-analyzed by triggering a time ramp with the beam pulse. At very early times it is shown that the time decay of the detected radiation should follow the time decay of the number of photons within a slablike region that can be seen by the detector. At late times the time behavior of the observed radiation is just that of Holstein's lowest eigenmode for pressure regions where the Holstein-Biberman equation holds (i.e., very low or relatively high pressure). The slit length for entrance to the spectrometer is set so that the slablike region that can be seen by the spectrometer has a dimension y_0 perpendicular to the cylindrical axis of such magnitude that at both very low and relatively high pressure the late and early values of $-(d/dt)\ln I$, where I is the rate of photon detection, are nearly equal. In this way one hopes that $(d/dt)\ln I$ does not change so rapidly that an estimate for the early-time decay is difficult to measure. It is found that this experimental device leads to almost constant values for $(d/dt)\ln I$, i.e., I decays exponentially with time.

The experimental data are compared with theory for the pressure range $0.0014 < P < 9$ Torr. The agreement with theory is reasonable except for $0.02 < P < 0.15$ Torr, where one expects the Jefferies and White approximation[15] to be poor. It is argued that the discrepancy in the latter region is less when one carries out a more complete solution of the transport equation not employing the Jefferies-White simplification. Better than 20% agreement between theory and experiment is difficult to obtain because of uncertainties in

the natural lifetime, the geometry of observation, and the initial excitation conditions.

In the range $0.005 < P < 0.25$ Torr, the value of $\beta_0 = -(d/dt)\ln I$ determined from a full solution of the Holstein-Biberman equation with the absorption coefficient $k(x)$ given by

$$k(x) = \frac{k_0 a}{\pi} \int_{-\infty}^{\infty} \frac{e^{-y^2}\,dy}{a^2 + (x-y)^2} \equiv k_0 H(a,x), \qquad (1)$$

and the emission profile (emission and absorption profiles are the same in a strict complete redistribution theory), given by

$$\phi(x) = \frac{a}{\pi^{3/2}} \int_{-\infty}^{\infty} \frac{e^{-y^2}\,dy}{a^2 + (x-y)^2} = \pi^{-1/2} H(a,x), \qquad (2)$$

is everywhere larger than the experimental value by at least a factor of 2. In the above,

$$k_0 = \frac{\lambda_0^3 N\gamma}{8\pi^{3/2}V_0}\,\frac{g_2}{g_1}, \quad a = \frac{\lambda_0\gamma}{4\pi V_0}\left(1 + \frac{\gamma_c}{\gamma}\right),$$

$$\frac{\gamma_c}{\gamma} = 0.904\,\frac{g_2}{g_1}\,\frac{N\lambda_0^3}{6\pi^2} \text{ (Ref. 17)}, \qquad (3)$$

$$x = (c/V_0\nu_0)(\nu - \nu_0), \quad V_0 = (2k_B T/m)^{1/2},$$

where k_B is the Boltzmann constant, T is the absolute temperature, c is the speed of light, m is the atomic mass, N is the number of atoms per unit volume, γ is the reciprocal of the natural lifetime for the resonance transition, λ_0 is the wavelength at the line center, ν_0 is the frequency at the line center, ν is the frequency, and g_2 and g_1 are the statistical weights of the upper and lower levels, respectively.

II. TRANSPORT EQUATION

The transport equation which will now be derived is based to a large extent on ideas that have been used for steady-state situations in astrophysics for several years.[11,12,14-16,18] In fact, an equation that is equivalent to ours for the steady state has been studied in several limiting cases by Hummer.[18] However, the incorporation of time dependence in the transport theory in the presence of partially (or completely) coherent scattering in the rest frame of the atom involves conceptual difficulties, and the resulting equation should be considered with this in mind.

We define a version of the frequency redistribution function[11,12] $R(x', \hat{n}', x, \hat{n})$ so that $R(x', \hat{n}'; x, \hat{n}) \times dS\bar{k}\,dx\,d\Omega$ represents the probability of a photon of frequency x' traveling in direction $\hat{n}'$ being absorbed while traversing a distance dS and being reemitted into solid angle $d\Omega$ about $\hat{n}$ with frequency in dx at x. Here $\bar{k} = \int_{-\infty}^{\infty}k(x)dx$. We also assume that the angular distribution of photons from a volume element dV' is isotropic and that the number of photons emitted in dx' at x' from dV' at $\vec{r}'$ in time dt is given by $dV'\,\gamma dtN(\vec{r}', x't) \times dx'$, where γ is the reciprocal natural lifetime of the excited state and $N(\vec{r}, x, t)dx\,dV$ is the number of excited atoms in dV at $\vec{r}$ at time t which will emit photons into dx at x. One expects that the photons absorbed in a volume element come nearly equally from all directions for strong resonance trapping and, therefore, emission is approximately isotropic. The assumption would follow even more directly if R itself were rather insensitive to the angle between $\hat{n}$ and $\hat{n}'$. The other assumptions, such as equating conceptually scattering and absorption and the assumption that $dV'\gamma dtN(\vec{r}', x', t)dx'$ represents the number of photons emitted in dt from dV into interval dx', are intuitive and theoretical justification will await a complete quantum-mechanical treatment of the problem. Applying the definitions of R and N and making use of the other assumptions, we obtain

$$\frac{\partial N}{\partial t}(\vec{r},x,t) = -\gamma N(\vec{r},x,t) - AN(\vec{r},x,t) + S(\vec{r},x,t) + \gamma\bar{k}\int_{-\infty}^{\infty}dx'\int_V dV'\,\frac{N(\vec{r}',x',t)\bar{R}(x',x)}{4\pi|\vec{r}-\vec{r}'|^2}$$

$$\times \exp\{-|\vec{r}-\vec{r}'|[k(x')+l^{-1}]\}, \qquad (4)$$

where γ is the reciprocal natural lifetime and A is the rate constant for collisions that convert the excitation energy to other forms; $S(\vec{r},x,t)$ is the number of excited atoms which will emit in the unit interval at x per volume per time created by processes other than absorption of photons from other parts of the system; $\bar{R}(x',x) = \int_{4\pi}d\Omega \times R(x',\hat{n}'; x,\hat{n})$; and l is the mean free path for photoabsorption by impurity atoms or by any process that intercepts photons in flight and converts the energy to another form.

We assume a very small concentration of excited atoms so that collisions between excited atoms as well as stimulated emission can be neglected. We have also assumed that the dimensions of the container are of the order of a few centimeters and that there is strong resonance trapping so that a large fraction of the emitted

photons have mean free paths considerably less 1 cm. Thus, the average flight time is less than 10^{-11} sec, and it is usually a good approximation [as was done in Eq. (4)] to neglect the time of flight compared with $1/\gamma$. It was further assumed that V is simply connected and that the bounding surface is convex. It has been assumed that temperature and density are such that interference effects can be neglected. Further, the line must be well isolated in frequency.

III. LOW-PRESSURE LIMIT

In this section several limiting cases will be considered. We begin with the case where the dimensions of the system are so large that few photons escape from the system during the first several natural lifetimes. Let us assume that $A = 0$ and $S = F(\vec{r}, x)\delta(t)$. Neglecting escape from V and integrating over V, we find

$$\frac{\partial N}{\partial t}(x, t) = -\gamma N(x, t) + \gamma \int_{-\infty}^{\infty} dx' N(x', t)$$

$$\times \bar{R}(x', x)[\phi(x')]^{-1}, \quad (5)$$

for $t > 0$. In Eq. (5), $N(x, t) = \int_V N(\vec{r}, x, t) dV$ and $\phi(x')$ is the absorption profile. Note that $N(t)$ $= \text{const} = \int_{-\infty}^{\infty} N(x, t) dx$, and that a steady-state solution to Eq. (5) is $N(x, t) = N(0)\phi(x)$. If one does indeed approach this steady state, then emission (when averaged over several successive emissions and absorptions or over space) has the same profile as absorption. We have used

$$\int_{-\infty}^{\infty} dx' \bar{R}(x', x) = \phi(x). \quad (6)$$

The last result is not dependent on the very low pressure assumption, but is general.

At very low pressures, one has coherent scattering in the rest frame of the atom and the wings of the absorption profile are unimportant. In this case, Unno[11] has shown that

$$\bar{R}(x', x) = \tfrac{1}{2} \operatorname{erfc}(\max(|x|, |x'|)) \quad (7a)$$

and

$$\phi(x) = e^{-x^2} \pi^{-1/2}, \quad (7b)$$

where $\operatorname{erfc}(x)$ is the complement of the error function. The time scale over which one approaches the steady-state solution $N(x, t) \simeq N(0)\phi(x)$ will now be established. Equation (5) when combined with (7a) and (7b) is equivalent to the partial differential equation

$$\frac{\partial^2}{\partial x^2}\left[\frac{\partial N}{\partial t}(x, t) + \gamma N(x, t)\right] + 2x \frac{\partial}{\partial x}\left(\frac{\partial N}{\partial t}(x, t) + \gamma N(x, t)\right)$$

$$= -2\gamma N(x, t). \quad (8)$$

Defining $\langle x^n \rangle$ by

$$N(0)\langle x^n \rangle = \int_{-\infty}^{\infty} x^n N(x, t) dx, \quad (9)$$

we find from Eq. (8)

$$\frac{d\langle x^n \rangle}{dt} = -\frac{n}{n+1} \gamma \langle x^n \rangle + \frac{n(n-1)}{2(n+1)}$$

$$\times \left[\frac{d\langle x^{n-2} \rangle}{dt} + \gamma \langle x^{n-2} \rangle\right]. \quad (10)$$

We find

$$\langle x \rangle = \langle x \rangle(0) e^{-\gamma t/2}, \quad (11a)$$

$$\langle x^2 \rangle = \tfrac{1}{2} + [\langle x^2 \rangle(0) - \tfrac{1}{2}] e^{-2\gamma t/3}, \quad (11b)$$

$$\langle x^3 \rangle = [\langle x^3 \rangle(0) - \tfrac{3}{2}\langle x \rangle(0)] e^{-3\gamma t/4}$$

$$+ \tfrac{3}{2}\langle x \rangle(0) e^{-\gamma t/2}, \text{ etc.} \quad (11c)$$

Note that within a few natural lifetimes (unless the initial moments are indeed large) all odd moments decay to zero, while all even moments also decay to those of $\pi^{-1/2} e^{-x^2}$. Thus, the decay to the steady state occurs very rapidly with most initial conditions.

Now consider the case where one initially has excited atoms at the center of a slab of thickness y_0. Further, take $\bar{R}(x', x)$ and $\phi(x)$ to be given by Eqs. (7a) and (7b). Equation (4) with $A = 0$ and $l = \infty$ becomes, for general $\bar{R}(x', x)$ and $\phi(x)$ and slab geometry $(d = \tfrac{1}{2} y_0)$,

$$\frac{\partial N}{\partial t}(y, x, t) + \gamma N(y, x, t)$$

$$= \tfrac{1}{2}\gamma \bar{k} \int_{-d}^{d} dy' \int_{-\infty}^{\infty} dx' \bar{R}(x', x)$$

$$\times E_1(k(x')|y - y'|) N(y', x', t), \quad (12)$$

where

$$E_n(z) = \int_1^{\infty} du\, e^{-zu} u^{-n}. \quad (13)$$

We choose x_1 so that $E_2[\tfrac{1}{2}k(x_1)y_0] < 10^{-5}$, or x_1 $= [\ln(\tfrac{1}{18} k_0 y_0)]^{1/2}$. Thus, if $\tfrac{1}{2} k_0 y_0 \gtrsim 50$, we can make simplifications as follows. First, define $N_0(y, x, t)$ and $N_1(y, x, t)$ as

$$N(y, x, t) = N_0(y, x, t), \quad |x| < x_1$$
$$= N_1(y, x, t), \quad |x| \geq x_1. \quad (14)$$

For $|x| < x_1$ a photon has almost no chance of tra-

versing a sizeable fraction of $\frac{1}{2}y_0$ and hence contributes little to the transport process. (Recall that most of the transport occurs when photons are emitted with rather large values of $|x|$ so that they can make a large spatial hop. This part of the low-pressure problem is expected to be very

similar to what is encountered in the Holstein-Biberman theory, since for $|x| < x_1$ one expects that emission with a Gaussian profile is rather accurate.) Thus, we approximate for $|x'| < x_1$ with $\frac{1}{2}k(x')E_1[k(x')|y - y'|] \approx \delta(y - y')$, and find for $|x| < x_1$,

$$\frac{\partial N_0}{\partial t}(y, x, t) = -\gamma N_0(y, x, t) + \gamma \int_{-x_1}^{x_1} dx' \bar{R}(x', x) N_0(y, x', t)(\phi(x'))^{-1}$$

$$+ \frac{1}{2}\gamma \int_{x_1}^{\infty} dx'(\phi(x'))^{-1}\mathrm{erfc}(x') \int_{-d}^{d} E_1(k(x')|y - y'|)N_1(y', x', t)k(x')dy'. \tag{15}$$

For $|x| > x_1$, Eq. (12) becomes

$$\frac{\partial N_1}{\partial t}(y, x, t) = -\gamma N_1(y, x, t) + \gamma \,\mathrm{erfc}(|x|) \int_0^{x_1} \frac{N_0(y, x', t)dx'}{\phi(x')}$$

$$+ \gamma \int_{x_1}^{\infty} dx' \frac{\mathrm{erfc}(\bar{x})}{2\phi(x')} \int_{-d}^{d} E_1(k(x')|y - y'|)N_1(y', x', t)k(x')dy', \tag{16}$$

where $\bar{x} = \max(|x|, |x'|)$. We expect that with the assumed $\bar{R}(x', x)$ that a photon emitted with $|x| > x_1$ will be absorbed and reemitted with $|x| > x_1$ only rarely and that two successive absorptions and reemissions in this frequency range are even more unlikely. If a photon is absorbed after being emitted with $|x| > x_1$, it will usually get reemitted at $|x'| < x_1$. Furthermore, the larger part of the photons emitted at $|x| > x_1$ were absorbed at $|x'| < x_1$ [as represented by the rather large $\mathrm{erfc}(|x|)$ $\times \int_0^{x_1} N_0(y, x', t)dx'/\phi(x')$ term]. For the above reasons the time behavior of $N_1(y, x, t)$ must be very similar to that of $N_0(y, x, t)$ and thereby in the large $\frac{1}{2}k_0 y_0$ limit, $|\partial N_1/\partial t| \ll \gamma N_1$. Thus, a good approximation should be obtained by neglecting $\partial N_1(y, x, t)/\partial t$ in at least the lowest-order approximation. It should be noted, however, that without the large source term involving $N_0(y, x, t)$ the neglect of $\partial N_1/\partial t$ could never be a good approximation. We obtain

$$N_1(y, x, t) = \mathrm{erfc}(|x|) \int_0^{x_1} \frac{N_0(y, x', t)dx'}{\phi(x')}$$

$$+ \int_{x_1}^{\infty} \frac{dx' \,\mathrm{erfc}(\bar{x})}{2\phi(x')} \int_{-d}^{d} E_1(k(x')|y - y'|)$$

$$\times N_1(y', x', t)k(x')dy'. \tag{17}$$

Using Eq. (17) we can easily solve for $N_1(y, x, t)$ in terms of $N_0(y, x, t)$. Let the linear integral operator $\hat{L}$ be defined so

$$\hat{L}F = \int_{x_1}^{\infty} dx' \frac{\mathrm{erfc}(\bar{x})}{2\phi(x')} \int_{-d}^{d} E_1(k(x')|y - y'|)$$

$$\times F(y', x')k(x')dy'. \tag{18}$$

Equation (17) becomes

$$N_1 = S_0 + \hat{L}N_1, \tag{19a}$$

where

$$S_0 = \mathrm{erfc}(|x|) \int_0^{x_1} \frac{N_0(y, x', t)dx'}{\phi(x')} \tag{19b}$$

Then, an adequate solution to Eq. (17) for $\frac{1}{2}k_0 y_0$ > 100 (it is less accurate for $\frac{1}{2}k_0 y_0 \approx 50$ but is still in the ball park) is

$$N_1 = (1 - \hat{L})^{-1}S_0 \approx (1 + \hat{L} + \hat{L}^2)S_0. \tag{20}$$

From Eq. (15) we see that $N_0(y, x, t)$ satisfies the partial differential equation

$$\left(\frac{\partial^2}{\partial x^2} + 2x\frac{\partial}{\partial x}\right)\left(\frac{\partial}{\partial t} + \gamma\right)N_0(y, x, t) = -2\gamma N_0(y, x, t), \tag{21}$$

with the subsidiary conditions that the y and t dependence be such that Eqs. (15) and (17) are satisfied. In the case of Eq. (5) a solution to the partial differential equation of Eq. (8) with the proper initial conditions satisfies Eq. (5) also; but in the case of Eq. (15) there is an x independent term on the right-hand side, and only certain solutions to Eq. (21) satisfy Eq. (15) with $N_1(y, x, t)$ chosen through Eq. (20).

We know that in an infinite medium the frequency dependence of N integrated over the spatial coordinates approaches a Gaussian in a few natural lifetimes (with the exact relaxation depending on how the gas was initially excited). In the case of a finite medium with $\frac{1}{2}k_0 y_0 > 100$, we expect that in an even shorter period of time the frequency

dependence at $|x| < x_1$ will approach a form very similar to that for an infinite medium. The time scale is faster because in a finite medium photons initially emitted on the far wings escape with a high probability, whereas in an infinite medium several emissions and absorptions are required to reduce these photon frequencies to an almost Gaussian emission profile. Thus, after a period of time that is no more than a few natural lifetimes (and may be zero for proper methods of excitation), the rate of escape of photons from the container becomes very slow and thus $|\partial N(y, x, t)/\partial t| \ll \gamma N(y, x, t)$. At such "late" times the solution of Eq. (21) corresponding to the above situation is easily shown to be

$$N_0(y, x, t) = F(y, t) e^{-x^2} \pi^{-1/2} + \gamma^{-1} \frac{\partial F}{\partial t}(y, t)$$
$$\times U(x, 0) + O\left(\gamma^{-2} \frac{\partial^2 F}{\partial t^2}(y, t)\right), \quad (22)$$

where

$$U(x, \alpha) = -\frac{2}{\pi} \int_0^\infty z^\alpha e^{-z^2} \ln z \cos(2xz) \, dz. \quad (23)$$

Many properties of $U(x, \alpha)$ and related functions are derived in the Appendix. By using these properties, we can show that use of $N_0(y, x, t)$ as defined by Eq. (22) causes all of the x dependence in Eq. (15) to disappear, provided that terms of the order of $\gamma^{-2} \partial^2 F(y, t)/\partial t^2$ are neglected.

The equation for $F(y, t)$ which remains, once Eqs. (22) and (19) are used in Eq. (15), is

$$\frac{\partial F}{\partial t}(y, t) + \gamma \left(\frac{g(x_1)}{h(x_1)}\right) F(y, t)$$
$$= \frac{\gamma x_1}{h(x_1)} \int_{-d}^{d} M(y, y') F(y', t) \, dy', \quad (24)$$

where

$$g(x_1) = \pi^{-1/2} e^{-x_1^2} - x_1 \operatorname{erfc}(x_1),$$

$$h(x_1) = U(x_1, 0) + g(x_1) + \tfrac{1}{2}\sqrt{\pi} \, e^{x_1^2} \operatorname{erfc}(x_1) \frac{\partial U(x_1, 0)}{\partial x},$$

$$M(y, y') = W(y, y', x_1),$$

and $W(y, y', x)$ satisfies

$$W(y, y', x) = \tfrac{1}{2}\overline{k} \int_{x_1}^{\infty} dx' \operatorname{erfc}(\overline{x}) E_1(k(x')|y - y'|) \operatorname{erfc}(x') + \tfrac{1}{2}\overline{k} \int_{x_1}^{\infty} dx' \operatorname{erfc}(\overline{x}) \int_{-d}^{d} E_1(k(x')|y - y''|) W(y'', y', x') \, dy''.$$

$$(25)$$

As implied earlier [i.e., Eq. (19)], three terms in an iterative solution of Eq. (25) are sufficient. In arriving at Eq. (24) some rather complicated looking terms which are linear in $\partial F(y, t)/\partial t$ have been neglected. The terms in question can be shown to be very small and, in fact, are little larger than corrections which would arise due to including the previously neglected $\partial N_1/\partial t$ of Eq. (16) as part of the next step in an iterative scheme.

Equation (24) does not involve the frequency variable x except in the evaluation of $M(y, y')$. The elimination of x yields a considerable simplification over Eq. (12). We now present a simple argument which, when coupled with work by Klots and Anderson,[8] Holstein,[5] Hummer,[18] Jefferies and White,[15] and others, makes it clear that for large $\tfrac{1}{2} k_0 y_0$ the escape of resonance photons from a slab can be calculated (except possibly at very early times) on the basis of a complete redistribution assumption. That is, the time behavior of solutions of Eq. (24) are very similar to solutions of the Holstein-Biberman equation.

Before going any further, it should be pointed out that physically one expects the solution of Eq.

(24) to be insensitive to the exact value chosen for x_1. We also note that if one simply assumes complete redistribution in frequency, the resulting Holstein-Biberman equation can be put in a form which is similar to Eq. (24). Thus,[5]

$$\frac{\partial N}{\partial t}(y, t) + \gamma N(y, t) = \gamma \int_{-d}^{d} T(|y - y'|) N(y', t) \, dy', \quad (26)$$

with

$$T(|y - y'|) = \pi^{-1/2} \int_0^\infty e^{-x'^2} E_1(k(x')|y - y'|)$$
$$\times k(x') \, dx',$$

$$\approx \operatorname{erf}(x_1) \delta(y - y') + T_1(|y - y'|),$$

where

$$T_1(|y - y'|) = \int_{x_1}^{\infty} \pi^{-1/2} e^{-x'^2} E_1(k(x')|y - y'|)$$
$$\times k(x') \, dx'.$$

Equation (25) becomes

$$\frac{\partial N}{\partial t}(y, t) = -\gamma \operatorname{erfc}(x_1) N(y, t)$$

$$+ \gamma \int_{-d}^{d} T_1(|y - y'|) N(y', t) dy'. \qquad (27)$$

Equation (27) is obviously equivalent to Eq. (24) in one physically unlikely case, that of very large x_1. In this limit,

$$\frac{g(x_1)}{h(x_1)} \approx \operatorname{erfc}(x_1)[1 + O(x_1^{-2})].$$

Further,

$$[x_1/h(x_1)] M(y, y') = [1 + O(x_1^{-2})] T_1(|y - y'|).$$

In the subtracted equations the integral operator term and the term in $N(y, t)$ [or $F(y, t)$ for Eq. (24)] do not largely cancel each other as in the case of Eq. (26) where the two terms on the right-hand side are often equal to a few parts in a thousand. For the latter reason, the $O(1/x_1^2)$ terms can be neglected within a few percent accuracy for $x_1 > 4$ or so. The result is that the equations for $F(y, t)$ and $N(y, t)$ become the same. However, situations with $x_1 > 4$ are rare in the no collision region, and further deviations from the $\bar{R}(x', x)$ have become important in most cases long before $x_1 > 4$.

We will now carry out a rather simple calculation that will demonstrate the fact that solutions to Eqs. (24) and (26) have very similar behavior as a function of time. We simplify as follows: (i) Assume that the gas was excited in such a way that Eq. (24) is valid from $t = 0$; (ii) we restrict ourselves to very early times so that as a rough approximation we can take

$$F(y', t) \approx \delta(y') F(t).$$

For $\frac{1}{2} k_0 y_0 \gtrsim 100$ there is a period of time of the order of 30 natural lifetimes during which the δ-function approximation of $F(y', t)$ represents a reasonably good approximation. With these simplifying assumptions, Eq. (24) becomes

$$\frac{dF}{dt}(t) = -\beta F(t),$$

where

$$\beta = \frac{\gamma}{h(x_1)} \left[g(x_1) - x_1 \int_{-d}^{d} M(y, 0) dy \right]. \qquad (28)$$

The early-time decay rate can also be calculated on the basis of Eq. (26) with the result

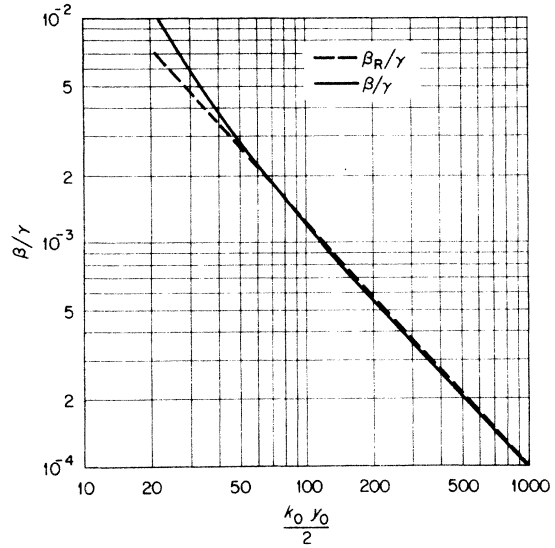$$\frac{dN}{dt}(t) = -\beta_R N(t), \qquad (29)$$

FIG. 1. Early-time decay constant vs optical depth at the center of the line in the low-pressure limit (β_R with complete redistribution, β without complete redistribution).

with

$$\beta_R = 2\gamma \pi^{-1/2} \int_0^\infty e^{-x^2} E_2(k_0 y_0 \tfrac{1}{2} e^{-x^2}) dx. \qquad (30)$$

Decay rates based on Eqs. (28) and (30) are within 4% for $\frac{1}{2} k_0 y_0 > 50$. Figure 1 shows the graphs of β and β_R as functions of $\frac{1}{2} k_0 y_0$. It should be noted also that the Holstein approximation to β_R lies almost 10% higher than is obtained by a more precise evaluation of Eq. (30).

The agreement between Eqs. (28) and (30) is remarkable and to a certain extent accidental for $\frac{1}{2} k_0 y_0$ as small as 50. In the complete redistribution in frequency approximation almost 10% more photons are emitted at frequencies such that $\frac{1}{2} k(x) y_0 < 1$ [i.e., at $|x| > (\ln(\frac{1}{2} k_0 y_0))^{1/2} = x_L$]. However, the resulting increase in β_R over β is almost exactly compensated for by the fact that when $|x| > x_L$ and Eqs. (7) are obeyed, there is a probability (typically of the order of 10%) that if the photon is absorbed with $|x| > x_L$, it will again be emitted with $|x| > x_L$ and hence stand an excellent chance of escaping. Successive emissions at large $|x|$ almost never occur with complete redistribution.

IV. FREQUENCY REDISTRIBUTION FUNCTION

Work by Zanstra,[14] Huber,[13] and others[18] suggests that $\bar{R}(x', x)$ is of the form

$$\bar{R}(x', x) = P_c R_1(x', x) + (1 - P_c) R_{II}(x', x), \qquad (31)$$

where $P_c = \gamma_c/(\gamma + \gamma_c)$ is the probability that colli-

sions will destroy the correlation between absorbed and emitted frequencies in the rest frame of the atom.

In the case of resonance broadening, $R_I(x', x)$ corresponds approximately to complete redistribution. That is,

$$R_I(x', x) \approx \phi(x') \phi(x), \qquad (32)$$

where $\phi(x)$ is the Voigt form of the absorption profile. This $R_I(x', x)$ is not exact for resonance broadening, but it becomes more precise as P_c increases toward unity and the probability of non-radiative transfer of the energy to another atom (before emission) with an uncorrelated velocity becomes close to unity.[5] However, even for smaller P_c where the probability of the energy hopping to another atom before reemission is smaller (and correlations between absorbed and emitted frequencies consequently exist), we still obtain $R_I(x', x) \simeq \phi(x') \phi(x)$ if either $|x'|$ or $|x|$ is large enough for the wings of the Lorentzian to dominate the Doppler effect.

For foreign-gas broadening, the resonance hopping process described above does not occur, and consequently x' and x are correlated to a greater extent because photons of a particular frequency are absorbed most strongly by atoms which "see" the photon to have $\nu = \nu_0$ in the atom's rest frame.

For small $|x'|$, the absorbing atoms do not have a Maxwellian distribution of velocities, and there is a resulting correlation between x' and x owing to the Doppler effect. However, for large $|x|$ and $|x'|$ the Doppler effect plays no part in absorption and little part in emission and again $R_I(x', x)$ $= \phi(x') \phi(x)$. At high pressures where the wings dominate the transport process we can use $R_I(x', x) = \phi(x') \phi(x)$ for foreign-gas broadening. In all subsequent parts of the present paper we will use $R_I(x', x) = \phi(x') \phi(x)$. The reader should, however, keep in mind the limitations associated with this approximation.

$R_{II}(x', x)$ is given by[18]

$$R_{II}(x', x) = \pi^{-3/2} \int_{|x-x'|/2}^{\infty} du\, e^{-u^2}$$
$$\times (\tan^{-1} W_1 - \tan^{-1} W_2), \qquad (33)$$

with

$$W_1 = [u + \min(x, x')]/a, \quad W_2 = [\max(x, x') - u]/a,$$

$$\gamma_c/\gamma = 0.904 N \lambda_0^3 (g_2/g_1)/6\pi^2 \quad \text{(Ref. 17)}.$$

The function $R_{II}(x', x)$ is the angle-averaged frequency redistribution function which would correspond to absorption with a Lorentzian profile in the atom's rest frame with coherent reemission

in the rest frame.

Equation (31) suggests a picture of the scattering process. Consider all photons absorbed at x'; for a fraction P_c of these, collisions will occur with the result that the reemitted photons are uncorrelated in frequency with the absorbed ones. However, for a fraction $1 - P_c$, no decorrelating collisions occur before emission, and the emitted photon has the absorbed frequency in the atom's rest frame.

The only quantum-mechanical work on $\bar{R}(x', x)$ is due to Huber.[13] The Huber theory is for foreign-gas broadening, but we believe that with our modification of γ_c and of $R_I(x', x)$ a similar relation should hold for self-broadening. In any case, Eq. (31) represents our best guess for a proper $\bar{R}(x', x)$ at relatively low pressures.

In the limit $P_c \approx 1$ there is complete redistribution in frequency, and the Holstein-Biberman equation follows from Eq. (5). In the limit $P_c \approx 0$ and at pressures such that the wings of the Voigt profile are unimportant, the limiting case studied in Sec. III is obtained. We have seen that in both of these limiting cases the Holstein-Biberman equation is a good approximation. Thus, it is tempting to guess that is is valid at intermediate pressures as well. However, we will presently show that there is an intermediate pressure region for gases with very large γ, fairly low temperature, and a restricted range of container dimensions where the approximation of complete redistribution in frequency is extremely poor.

We begin by noting that $R_{II}(x', x)$ can be written as follows[15,18] (see Fig. 2):

$$R_{II}(x', x) = \tfrac{1}{2} b(x', x) \operatorname{erfc}(\bar{x})$$
$$+ a(x', x)\, \phi(x') \pi^{-1/2} e^{-(x-x')^2}, \qquad (34)$$

where $\bar{x} = \max(|x|, |x'|)$. Define x_c by $e^{-x_c^2} = a\pi^{-1/2}$ $\times x_c^{-2}$. If $|x'| << x_c$, then $b(x', x) \approx 1$ and $a(x', x) \approx 0$. If $|x'| >> x_c$, we have $b(x', x) \approx 0$ and $a(x', x) \approx 1$. As a function of $|x'|$, $b(x', x)$ drops from near unity to zero near x_c with the rate of change depending somewhat on $|x|$. Correspondingly, $a(x', x)$ rises from near zero to unity for $|x'|$ near x_c, the rate of rise depending somewhat on $|x|$. It should be pointed out that at large $|x'|$, Eq. (34) with $b(x', x)$ $= 0$ and $a(x', x) = 1$ is approximate in the sense that the x dependence is peaked at x' but is slightly skewed toward smaller $|x|$. However, the Gaussian is a good approximation. For $|x'|$ considerably less than x_c, redistribution occurs almost as if there were no wings on the absorption profile. With $|x'|$ much greater than x_c, the motion of the atoms has little to do with the absorption process since there are so few atoms with velocities large enough to effect absorption appreciably by way of
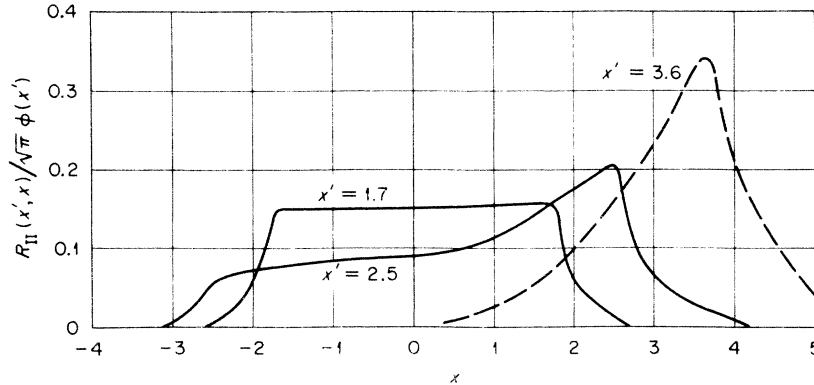
FIG. 2. Frequency redistribution function corresponding to absorption with a Lorentzian profile in the rest frame of the atom followed by coherent emission (appropriate for the 1048-Å resonance line of argon at 293 °K at pressure less than 10 Torr).

the Doppler effect.[15] Most of the absorption should be due to the more plentiful low-velocity atoms with the only mechanism for redistribution in frequency being the rather slight Doppler shifts occurring due to their motion. Thus, the x dependence is the Gaussian about $x = x'$.

We note the following about the function $R_{II}(x', x)$.

(a) A photon absorbed with $|x'| < x_c$ and reemitted without a decorrelating collision having occurred gets redistributed almost uniformly over frequencies $-|x'| \lesssim x \lesssim |x'|$, and there is almost no probability of emission with $|x| > |x'| + 1$. Thus, there are no "wings" such as those present in the emission profile $\phi(x)$ when a decorrelating collision occurs. If P_c is significantly less than unity, but $\frac{1}{2} k_0 y_0$ is so large that most of the photons that escape must have $|x| \gtrsim x_c$, the assumption of complete frequency redistribution (so that emission has a Voigt profile) leads to a much greater rate of escape from the container than would arise from use of Eq. (31) in Eq. (4).

(b) Where P_c is significantly less than unity, but most of the escaping photons have $|x| > x_c$, there is another important difference from the complete redistribution case. This occurs because many photons emitted with $|x| \gg x_c$ get absorbed. If they are reemitted before a decorrelating collision occurs, they will, with high probability, again have $|x| \gg x_c$. Thus, a significant contribution to the transport and escape of the radiation will be made by photons that make two or more successive large spatial jumps. With complete redistribution, successive large spatial jumps are exceedingly improbable.

We can now write a condition for large deviations from a theory that assumes complete frequency redistribution. The condition is that $P_c = \gamma_c/(\gamma + \gamma_c)$ is significantly less than unity and yet

(note that large $k_0 y_0$ implies that few photons ever escape with $|x| < x_L$) $x_L = (\frac{1}{2} \ln k_0 y_0)^{1/2}$ is large enough so that the number of photons emitted with $|x| > x_L$ is significantly less than what would be emitted with $|x| > x_L$ if there were complete redistribution in frequency. We expect this condition to occur if P_c can be small and yet x_L be only slightly smaller (or even larger) than x_c. With complete redistribution for $|x| > x_L$, emission would be with a Voigt profile $\simeq \pi^{-1/2} e^{-x^2} + a/\pi x^2$, while with coherent scattering in the atom's rest frame, emission occurs without a wing term $a/\pi x^2$. Thus, escape will be much slower than with complete redistribution unless the area under the wing term beyond x_L is much smaller than the corresponding area under a Gaussian. Using the definition of x_L, we find that the conditions for large deviations from complete redistribution are

$$P_c < 0.7 \quad \text{and} \quad k_0 y_0 a \gtrsim 1, \tag{35}$$

where k_0 is the absorption coefficient at value line center and a is the width parameter in the Voigt profile, defined in Sec. I. Thus, very large values of $(y_0/v_0 \tau)(\lambda_0/v_0 \tau)$ are conducive to producing the deviations in question. The effect is enhanced by choosing large y_0, low temperature, and short natural lifetimes.

In cases where $x_L < x_c - 0.5$ and $\frac{1}{2} k_0 y_0 > 30$, the photons that are escaping have frequencies such that the wings of the absorption profile play no part. Further, almost all of the photons that are emitted have $|x| < x_c$ so that the entire transport process is independent of the presence of the wings on the absorption profile. In such a case we can simply use

$$\bar{R}(x', x) = \frac{1}{2}(1 - P_c) \operatorname{erfc}(\bar{x}) + P_c \pi^{-1} e^{-(x^2 + x'^2)}$$

and obtain correct results. Thus, while complete

redistribution in the strict sense [i.e., using $\bar{R}(x',x) = \phi(x)\phi(x')$] is not valid, we still get correct results with it for $x_L < x_c - 0.5$ if the wings are omitted on the absorption profile and as the results of Sec. III would suggest that $\frac{1}{2}\text{erfc}(\bar{x})$ can be replaced by $e^{-(x^2 + x'^2)}/\pi$. Therefore, we have as an approximation that leads to accurate escape rates, $\bar{R}(x',x) = e^{-(x^2 + x'^2)}/\pi$. Escape rates calculated from this form of $\bar{R}(x',x)$ are just those of the Holstein-Biberman theory for pure Doppler broadening.

V. EARLY-TIME DECAY OF
RESONANCE RADIATION

In this section we restrict ourselves to the problem of calculating the rate of escape of resonance radiation from a slab. We assume that at $t = 0$ all of the excited atoms are spread uniformly over the midplane and that the excitation is carried out in such a way that very few of the initially excited atoms emit photons with $|x| > x_L$. In this case we can use Eq. (12) along with Eqs. (31) and (34):

$$\frac{\partial N}{\partial t}(y,x,t) + \gamma N(y,x,t) = \gamma P_c \phi(x) \int_{-y_1}^{y_1} dy' \int_{-\infty}^{\infty} dx' \tfrac{1}{2} E_1(k(x')|y-y'|) N(y',x',t) k(x') + \gamma(1-P_c) \int_{-y_1}^{y_1} dy' \int_{-\infty}^{\infty} dx'$$

$$\times \frac{R_{II}(x',x)}{2\phi(x')} E_1(k(x')|y-y'|) N(y',x',t) k(x'). \tag{36}$$

In Eq. (36) the slab thickness is $2y_1$.

In two cases we can calculate the early-time escape rate from the region between $-\frac{1}{2}y_0 < y < \frac{1}{2}y_0$, where $\frac{1}{2}y_0 \lesssim y_1$. These are the following.

(i) $x_L < x_c - 0.5$. In this case the discussions of Secs. III and IV lead us to believe that while complete redistribution in its strictest sense may result in large errors, nevertheless the results of the Holstein-Biberman theory for pure Doppler broadening are correct.

(ii) Define x_E by $\frac{1}{2}k(x_E)y_0 = 1$. If $x_E > x_c + 3$ and also $P_c > 0.3$, we will presently see that great simplifications occur. In case (ii) the photons which dominate the transport process (i.e., have $|x| \gtrsim x_E$) almost always have one of the following properties: (a) a decorrelating collision occurred before emission of the photon; (b) the photon absorbed before emission had $|x'| > x_c + 2$. Now a photon that is emitted with $|x| \gtrsim x_E$ can either escape or be absorbed. If it is absorbed and no decorrelating collision occurs before emission, Eq. (34) shows that it will almost always be emitted with $|x - x'| \lesssim 1$. However, if it is absorbed and a collision does occur, the emitted photon has high probability of having $|x| < x_c - 1$. It is unlikely with our restrictions on P_c and x_E that more than three or four absorptions and reemissions will occur for a photon originally having $|x| > x_E$ before the energy either escapes or a collision occurs, returning the photon to a frequency with $|x| < x_c - 1$ on the next emission. Further, $k(x)$ varies slowly with x at $|x| \gtrsim x_c$. Thus, the accumulated change in frequency of a quantum while being absorbed and reemitted with $|x| > x_c + 3$ is small so that the same absorption coefficient can be used for all successive emissions with $|x| > x_c$. In cases where

decorrelating collisions occur, the spectrum of emitted photons having $|x| > x_E$ falls off very slowly with $|x|$ so that many of the photons which contribute to the transport process are emitted with $|x|$ considerably greater than x_E. We expect, then, that the transport process is described properly by replacing Eq. (34) with

$$R_{II}(x',x) = \tfrac{1}{2}b(x',x)\,\text{erfc}(\bar{x}) + a(x',x)$$
$$\times \phi(x')\delta(x-x'). \tag{37}$$

In the region where $b(x',x)$ is of significant magnitude we expect that we have complete redistribution (for $|x| \ll x_E$ the presence of the boundary does not effect the distribution of emitted frequencies greatly), and we can take

$$R_{II}(x',x) = b(x',x)\phi(x')\pi^{-1/2}e^{-x^2}$$
$$+ a(x',x)\phi(x')\delta(x-x'). \tag{38}$$

Since the approach of $R_{II}(x',x)$ to $\phi(x')\delta(x-x')$ at $|x| \gtrsim x_E$ together with the sum rule

$$\int_{-\infty}^{\infty} dx\, R_{II}(x',x) = \phi(x'), \tag{39}$$

are the important features of $R_{II}(x',x)$ (as far as correctly describing the transport process is concerned), we can take

$$b(x',x) = 1 - a(x',x) = \pi^{-1/2}e^{-x'^2}/\phi(x'), \tag{40}$$

and still retain qualitatively the right balance between completely coherent and completely incoherent scattering and satisfy the sum rule exactly. We will presently show that when $R_{II}(x',x)$ is simplified as described above, it becomes possible to determine the rate of escape of photons at small t with a minimum of difficulty.

Thus, we will use the following form of $R_{II}(x', x)$ in describing the early time escape of resonance photons from the region $-\frac{1}{2}y_0 < y < \frac{1}{2}y_0$ (Ref. 15):

$$R_{II}(x', x) \approx e^{-(x^2 + x'^2)}/\pi + [\phi(x') - \pi^{-1/2}e^{-x'^2}]\delta(x - x').$$

$$(41)$$

It should be noted further that when $x_L < x_c - 0.5$, escape rates calculated while using the $R_{II}(x', x)$ of Eq. (41) yield correct results. The reason is that $\phi(x) - \pi^{-1/2}e^{-x^2}$ is very small for $|x| < x_c - 0.5$,

and consequently the term involving $\delta(x - x')$ plays no significant part in this limiting case. Since Eq. (41) is expected to lead to correct escape rates at both low and relatively high pressures, we will carry out a calculation which uses it at all pressures. The region where the results should be accurate can then be estimated by using the above restrictions. The results will also be correct, of course, at pressures where P_c is so close to unity that approximations in $R_{II}(x', x)$ do not matter.

Combining Eqs. (36) and (41), we obtain

$$\frac{\partial N}{\partial t}(y, x, t) + \gamma N(y, x, t) = \gamma P_c \phi(x) \int_{-y_1}^{y_1} dy' \int_{-\infty}^{\infty} dx' \tfrac{1}{2} E_1(k(x')|y - y'|) N(y', x', t) k(x') + \gamma(1 - P_c) \pi^{-1/2} e^{-x^2}$$

$$\times \int_{-y_1}^{y_1} dy' \int_{-\infty}^{\infty} dx' \tfrac{1}{2} b(x') E_1(k(x')|y - y'|) N(y', x', t) k(x')$$

$$+ \gamma(1 - P_c) a(x) \int_{-y_1}^{y_1} dy' \tfrac{1}{2} E_1(k(x)|y - y'|) N(y', x, t) k(x).$$

$$(42)$$

Integrating both sides of Eq. (36) over x and y gives

$$\frac{dN}{dt}(t) = -\gamma \int_{-y_0/2}^{y_0/2} dy \int_{-y_1}^{y_1} dy' \int_{-\infty}^{\infty} dx' [\delta(y - y') - \tfrac{1}{2} E_1(k(x')|y - y'|) k(x')] N(y', x', t),$$

$$(43)$$

where

$$N(t) = \int_{-y_0/2}^{y_0/2} dy \int_{-\infty}^{\infty} dx \, N(y, x, t).$$

We need to determine a form of $N(y', x', t)$ which has the correct y' and x' dependence at very early times for those photons which have large $|x|$ and hence contribute to changing $N(t)$. Such a $N(y', x', t)$ can be used directly on the right-hand side of Eq. (43) for all y' and x' since little contribution to $dN(t)/dt$ will occur at $|x'| < x_B - 1$.

Note that those photons with $|x|$ somewhat greater than x_B seldom get reemitted with $|x| > x_B$ more than four times so that in the limit of strong imprisonment the time dependence of $N(y, x, t)$ for $|x| > x_B$ must follow that for $|x| < x_B$. There is essentially an instantaneous balance between absorption of photons emitted at $|x| > x_B$ by the very plentiful atoms that absorbed at $|x| < x_B$ but underwent a decorrelating collision and escaped to the walls along with incoherent emission. We evaluate Eq. (42) at $|x| \gtrsim x_B$ and note that all of the other terms are large compared with $\partial N(y, x, t)/\partial t$ in the strong trapping limit. Further, most of the contribution to the integrals in the terms representing complete redistribution come from small x so that at very early times

$$\tfrac{1}{2} \int_{-y_1}^{y_1} dy' \int_{-\infty}^{\infty} dx' \, E_1(k(x')|y - y'|) N(y', x', t) k(x')$$

$$\approx N(t)\delta(y)$$

and

$$\tfrac{1}{2} \int_{-y_1}^{y_1} dy' \int_{-\infty}^{\infty} b(x') dx' \, E_1(k(x')|y - y'|) N(y', x', t) k(x')$$

$$\approx N(t)\delta(y).$$

Thus, at large $|x|$ with strong imprisonment

$$N(y, x, t) \approx [P_c \phi(x) + (1 - P_c) \pi^{-1/2} e^{-x^2}]$$

$$\times N(t)\delta(y)$$

$$+ (1 - P_c) a(x) \int_{-y_1}^{y_1} dy' \tfrac{1}{2} E_1(k(x)|y - y'|)$$

$$\times N(y', x, t) k(x).$$

$$(44)$$

The "picture" associated with Eq. (44) is that at very early times most of the excited atoms remain near $y = 0$. When a photon is emitted that can traverse a significant distance without absorption, it either escapes or, if absorbed, is reemitted at the same frequency with a probability $(1 - P_c) a(x)$, and again can either escape or be absorbed, etc. The process continues for a small time until escape occurs or the photon undergoes

an incoherent emission which leads with a probability of nearly unity to an emitted photon with $|x| \ll x_E$. In the latter case many natural lifetimes pass (for $\frac{1}{2}k_0 y_0 > 50$) before an emission with $|x| \gtrsim x_E$ occurs again. While we can hardly ever neglect spatial transport before escape for photons absorbed at $|x| > x_E$, we can, for a short period of time, neglect the spatial spread of atoms emitting photons with $|x| < x_E$ since at least two nonsuccessive emissions at large $|x|$ must become probable before the corrections become important. It should also be pointed out that Eq. (44) assumes that $N(y, x, t)$ changes very little at any y or x during the time a photon remains at $|x| \gtrsim x_E$. Thus, again the requirement is that we must have strong imprisonment.

In dealing with Eq. (44) it is convenient to define $\overline{U}(\tau, \lambda)$ by

$$N(y, x', t) = k(x')[P_c \phi(x') + (1 - P_c) \pi^{-1/2} e^{-x'^2}]$$

$$\times N(t) \overline{U}(\tau, \lambda), \tag{45}$$

where $\tau = k(x')y$, $\tau' = k(x')y'$, $\tau_1 = k(x')y_1$, $\tau_0 = k(x')y_0$, and $\lambda = a(x')(1 - P_c)$. We can then show that

$$\overline{U}(\tau, \lambda) = \delta(\tau) + \frac{1}{2}\lambda \int_{-\tau_1}^{\tau_1} E_1(|\tau - \tau'|) \overline{U}(\tau', \lambda) d\tau'. \tag{46}$$

Defining β by

$$\frac{dN}{dt}(t) = -\beta N(t), \tag{47}$$

and using Eq. (45) on the right-hand side of Eq. (43), we obtain

$$\beta = \gamma \int_{-\infty}^{\infty} dx' [P_c \phi(x') + (1 - P_c) \pi^{-1/2} e^{-x'^2}]$$

$$\times \left[\lambda + (1 - \lambda) E_2(\tfrac{1}{2}\tau_0) - (1 - \lambda)\lambda^{-1} \int_{-\tau_0/2}^{\tau_0/2} g(\tau, \lambda) d\tau \right], \tag{48}$$

where

$$g(\tau, \lambda) = \overline{U}(\tau, \lambda) - \delta(\tau) - \lambda \tfrac{1}{2} E_1(|\tau|).$$

Equation (48) is rather general, holding for any $\tau_1 \geq \frac{1}{2}\tau_0$ subject to the restrictions specified earlier. However, we shall see in Sec. VI that the special case where $\tau_1 \gg \frac{1}{2}\tau_0$ is of particular importance in connection with the experiment concerning the 1048-Å resonance line of argon. When $\tau_1 > \frac{3}{2}\tau_0$ and $\lambda < 0.7$ for the larger portion of the escaping photons, we can let $\tau_1 \to \infty$. Then, using the method of Fourier transforms,

$$\lambda^{-1} \int_{-\tau_0/2}^{\tau_0/2} g(\tau, \lambda) d\tau = \frac{\lambda}{\pi} \int_{-\infty}^{\infty} P^{-1}[R(P)]^2$$

$$\times [1 - \lambda R(P)]^{-1} \sin(\tfrac{1}{2}P\tau_0) dP, \tag{49}$$

where

$$R(P) = [\tan^{-1}(P)]/P. \tag{50}$$

Thus, we have been able to reduce the calculation of the early time β to quadrature for the special case of $\tau_1 \to \infty$. It should be pointed out also that Eq. (46) is a much studied equation and is readily solved for finite τ_1.

In Sec. VI we combine Eqs. (48) and (49) in order to compare the theory with an experiment on the 1048-Å line of argon.

VI. EXPERIMENT

In this section an experiment is reported which examines the time behavior of the resonance trapping of the 1048-Å photons in argon. Argon atoms in a gas are excited along a nearly straight line by a pulsed beam of 2-MeV protons and the $^1P_1$ state serve as a source of resonance photons. The gas is contained in a narrow cylinder, and the distribution in time of escaping 1048-Å photons is examined over the pressure range 0.0015 to 10 Torr. The results are in substantial disagreement with values obtained by a direct application of the Holstein-Biberman theory, assuming strict complete redistribution in frequency (i.e., emission profile equals absorption profile).

Excitation of atomic levels by fast-charged particles provides an excellent method to study vacuum ultraviolet emission from noble gases. By this method Hurst and co-workers[10,19] have been able to obtain emission spectra which are quite reproducible. A beam of protons can be used to produce a clearly defined, initial spatial distribution of excited states, and it can be terminated after a few nanoseconds so that $t = 0$ is well defined. Well-defined initial conditions are essential for studies of the transport of resonance photons if critical comparisons with theory are to be made.

The 1048-Å emission of argon was chosen for this study for the following reasons: (i) The associated $^1P_1$ atomic level is easily excited by fast-charged particles owing to its large oscillator strength; (ii) the level has no complicated fine structure; (iii) the level is isolated in energy from other excited states; and (iv) the emitted 1048-Å photons are transmitted by a lithium-flouride window so that differential pumping is not required.

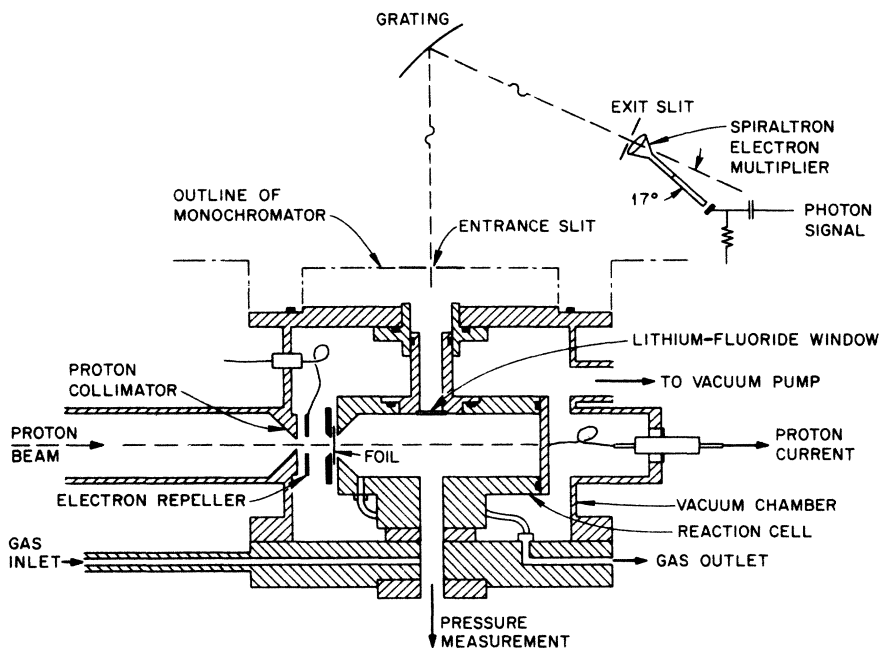Applying the conditions $P_c < 0.7$ and $k_0 y_0 a \gtrsim 1$

FIG. 3. Reaction cell and environs.

(see Sec. IV) to this resonance line in the present geometry (with $y_0 = 0.714$ cm), one obtains a pressure region $0.005 < P < 2$ Torr where the complete redistribution assumption should cause large errors. This wide pressure region is the result of the short natural lifetime ($\approx 2 \times 10^{-9}$ sec) of the $^1P_1$ level. *The much studied level in mercury which decays by emission at 2537 Å has an appreciably longer lifetime* (1×10^{-7} sec), *accounting for the lack of a similar pressure region.*

The apparatus used in this experiment is shown in Fig. 3. Argon gas flows continuously through the reaction cell. Bursts of 2-MeV protons (less than 20 nsec full width at half-maximum in duration) from a 3-MeV van de Graaff accelerator pass through a 3-mm collimating aperture, then enter the reaction cell through a 0.0001-in. Havar foil. The reaction cell is a stainless-steel cylinder 7 cm long with a radius of 1.11 cm. The protons are stopped by the back plate of the cylinder.

The resonance radiation which escapes to the walls of the cylinder may enter the dispersing monochromator via a 0.714-cm-diam cylindrical aperture halfway down the length of the cell. To prevent argon from flowing into the monochromator chamber, a lithium-flouride disk (about 1 mm thick) was placed across the aperture flush with the walls of the reaction cell. This precaution is not trivial, because pressure gradients along the escaping photon path would greatly complicate interpretation. Additional apertures were present

in the cell to facilitate gas flow and pressure measurements. To measure the proton current, it was necessary to electrically isolate the cell from the surrounding hardware.

The repetition period of the proton pulses was kept low enough to allow the effects of previous pulses to dissipate. Typically, this repetition period was 64 μsec, resulting in an average proton current of 0.06 μA.

Photons, on passing through the lithium-flouride window, were dispersed by a 50-cm McPherson model 235 scanning monochromator which employs a Seya-Namioka geometrical arrangement. Entrance and exit slits were 1 cm high. The monochromator chamber was maintained at a pressure of less than 10^{-6} Torr during the experiment. A Bendix spiraltron electron multiplier (SEM model 4219X), mounted directly behind the exit slit, was used to detect the photons. The cone of the SEM had a base diameter of 1.1 cm.

Pressure measurements in the reaction cell were made with an MKS baratron capacitance manometer (head type 77H-10). The lower pressure measurements should be accurate to ±0.5 μm. High-purity (99.999%) argon was used; the gas was allowed to flow to maintain purity.

A block diagram of the electronics is shown in Fig. 4. The time distribution of escaping resonance photons was determined by a single-photon counting technique as follows. A proton pulse, in passing through a time pick-off cylinder, induced
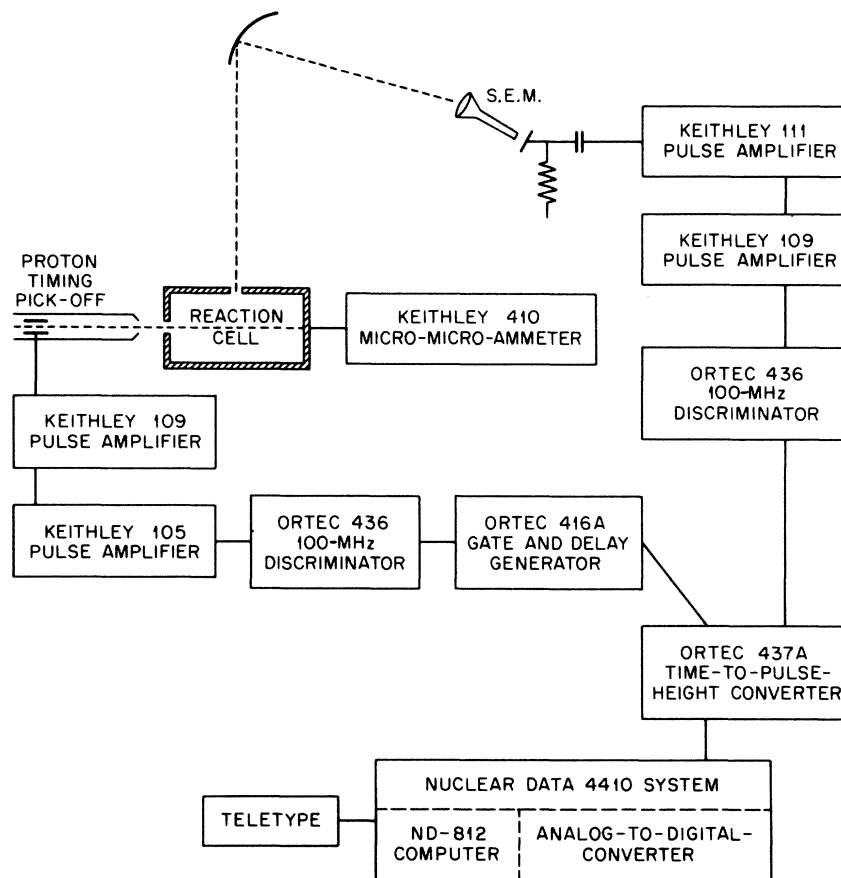
FIG. 4. Block diagram of the electronics.

a signal which was amplified and used as an input to the time-to-pulse-height converter (TPHC). Some of the photons, which escaped from the reaction cell into the proper solid angle and with the selected wavelength, triggered the SEM detector. These signals were then amplified and used as a second input for the TPHC. In the experiment, the ratio of photons detected to incident photon pulses ranged from 1:20 to 1:2000, so that the detection of a photon for any given proton burst was a rare event. The output signals from the TPHC were analyzed and stored by a multichannel analyzer. The number of counts plotted versus channel number gave the time distribution of the emitted photons relative to the time of incidence of a proton pulse. Figure 5 shows, on a ln scale, typical curves obtained after the SEM background count has been removed. The solid line represents an exponential function obtained by fitting to the early-time data. Additional information on the experimental apparatus and procedure is given in Ref. 20.

After many proton pulses, the number of counts

stored in the jth channel of the analyzer is given by

$$I(t_j)\Delta t = N_P \epsilon \Delta t \int dx \int_{V_F} dV \frac{\Delta\Omega}{4\pi} \gamma N(\vec{r}, x, t_j)$$

$$\times T(\vec{r}, x), \qquad (51)$$

where $\gamma N(\vec{r}, x, t_j) dx\, dV$ is the rate at time t_j at which photons with frequency between x and $x + dx$ are emitted from the volume element dV at $\vec{r}$; $T(\vec{r}, x)$ is the transmission factor, the probability that a photon of frequency x will traverse the distance from dV to the window (measured in the direction toward the detector) without being absorbed; and $\Delta\Omega/4\pi$ is the probability of this photon being emitted into the proper solid angle to reach the detector. Isotropic emission is assumed from each volume element. The SEM detector (1 cm high, 1 m away) subtends a very small solid angle at any volume element dV in the cell. The entire detector (as seen through the monochromator exit slit) is visible to each dV in V_F, enabling one to use the same solid angle for each.

N_p is a number proportional to the number of excited atoms produced per cm of track length during a given experiment; ϵ is the combination of transmission efficiency of window, reflection efficiency of grating, and detection efficiency of the SEM detector, evaluated at the line center; and V_F is the volume of the reaction cell "visible" to the SEM detector. The spatial integral in Eq. (51) is always carried out over V_F; the frequency integration is performed over the entire profile of the 1048-Å line. The volume of the reaction cell V_F viewed by the SEM detector is determined in the horizontal plane by the monochromator entrance-slit width z_0 and in the vertical plane by the diameter y_0 of the cylindrical aperture to the reaction cell [see Fig. 6(a)].

The fairly small value of y_0 (0.714 cm) compared to the reaction-cell diameter ($2R = 2.22$ cm) is important at early times (measured from the proton pulse) for two reasons: (i) With $y_0/2R \ll 1$, the escape of resonance photons from V_F is determined almost entirely by those photons which escape across the boundary of a region between two infinite parallel planes separated by the distance y_0; (ii) escape from this "slab" region is consistent with the assumptions used in the analysis of Secs. III and V. We now consider these points in more detail.
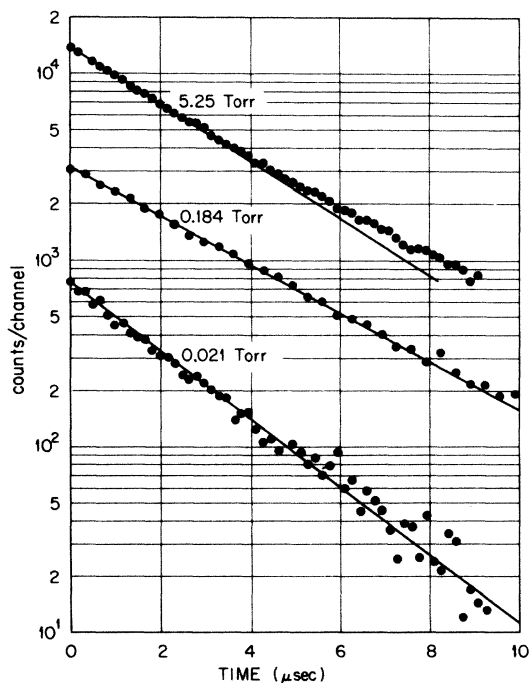
For a limited time after the proton pulse has traveled through the cylinder, a dominant fraction of the $^1P_1$ states is confined to a small region near the axis. Most of the photons are emitted with a frequency near the core of the resonance line and in the strong trapping limit ($\frac{1}{2}k_0 y_0 > 50$) are absorbed and reemitted many times before traversing a distance comparable with $\frac{1}{2}y_0$. Photons which escape from V_F generally, then, have been emitted from near the axis with frequency such that $|x| > x_L$. Escape from V_F in the z direction [see Fig. 6(b)] is not important owing to the cylindrical symmetry of $N(\vec{r}, x, t)$ about the proton beam. Further, there is a much larger probability for photons to escape across the sides of V_F parallel to the xz plane than through the ends [partially indicated by shaded area in Fig. 3(b)]. For purposes of calculating the number of excited atoms that can be seen, the volume of V_F can thus be extended to infinity in the positive and negative x and z directions with very little error introduced in evaluating Eq. (51). This error is estimated to be about 2% in the high- and low-pressure limits.

In Secs. III and V, photons emitted at frequencies less than some critical value x_0 (x_1 in Sec. III, x_c in Sec. V) are treated as if they were emitted and reabsorbed at $y = 0$. In the analysis it is assumed that the fraction of the number of excited states which will emit photons with $|x| > x_0$ is small compared to the fraction which will emit at $|x| < x_0$.

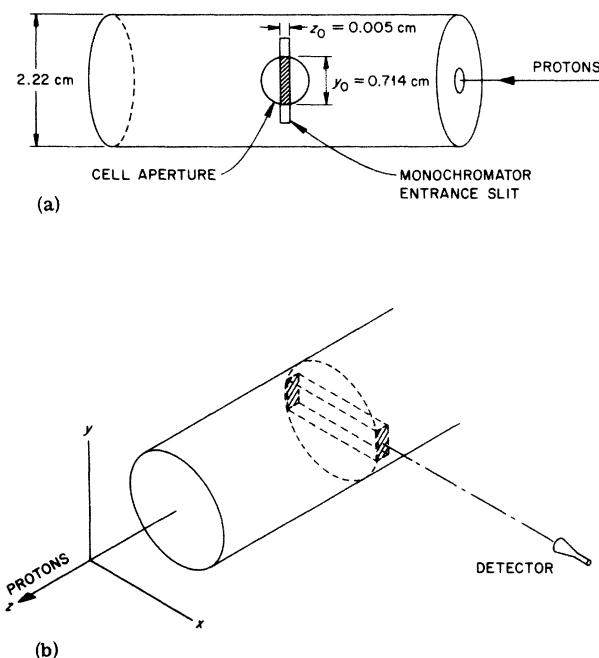FIG. 5. Decay curves for argon 1048-Å resonance radiation at several pressures.

FIG. 6. Reaction cell as viewed by the photon detector. (a) Shaded area is in view of SEM detector. (b) Cross section of slab used in early time analysis.

Escape from the slab can occur only for those photons with $|x| > |x_0|$. Photons which are absorbed with $|x'| > x_0$ are allowed to move from $y = 0$, and, as there is (depending on the pressure) an appreciable probability of being reemitted with $|x| > x_0$, the analysis treats escape by correlated jumps in a realistic way. However, if after absorption at $|x'| > x_0$ the excited atom undergoes a decorrelating collision so that emission will most probably occur with $|x| < x_0$, this latter emission will be treated as if it occurred at $y = 0$. Hence, a subsequent emission at $|x| > x_0$ will be assigned an improper spatial location. This error is minimized if one considers only short enough times after the proton pulse that nonsuccessive emissions at $|x| > x_0$ are improbable (early times).

Then, at low pressures, $N_0(y, x, t)$ from Eq. (22) with time dependence described by Eq. (28) can be used to approximate $N(\vec{r}, x, t)$ in Eq. (51). Similarly, at intermediate pressures, Eqs. (44) and (48) can be applied. Within the early-time restriction, these substitutions into Eq. (51) should give accurate values for the time dependence of $I(t) \Delta t$. To evaluate the actual magnitude of $I(t) \Delta t$, one needs to redefine the transmission factor $T(\vec{r}, x)$ in terms of a function $T_1(R, x)$ which allows for escape to the window from the axis by successive emissions with $|x| > x_0$. The accuracy of the time dependence obtained under these conditions will be discussed further in the analysis of the data.

The experimental data for the time distribution

of escaping 1048-Å radiation were obtained over the pressure range 0.0015–9.3 Torr. This range is divided into three general regions determined by the dominant trapping process at that pressure. As mentioned earlier in this section, there should be a pressure range $0.0005 \lesssim P \lesssim 2$ Torr where the complete redistribution in frequency assumption fails. Figure 7 shows a plot of the quantities x_c, x_E, x_L versus pressure for slab geometry with $y_0 = 0.714$ cm (see Secs. IV and V for definitions). Note, for this experiment, $\frac{1}{2} k_0 y_0 = 12.1 \times 10^3 P$ and $P_c = 1.74P/(1 + 1.74P)$, where P is the argon pressure in Torr.

Below $P = 0.01$ Torr, the condition $x_L \lesssim x_c - 0.5$ is satisfied so the analysis of Sec. III applies at early times. Emission and absorption are described by Eqs. (7). However, the strong trapping requirement is only marginally satisfied at 0.0014 Torr.

In the intermediate pressure region ($0.005 < P < 2$ Torr), the analysis of Sec. V applies at early times. As discussed in Sec. V, one should expect good agreement between the calculated values and the experimental values in two situations: (i) $x_L < x_c - 0.5$; (ii) $x_E > x_c + 3$ and $P_c > 0.3$. From Fig. 7, condition (i) is satisfied below 0.01 Torr, and condition (ii) is satisfied above 0.28 Torr. In the pressure region $0.01 < P < 0.28$ Torr, one expects the approximation used in the analysis of Sec. V to predict photon escape rates which are too small, but the error is difficult to estimate.

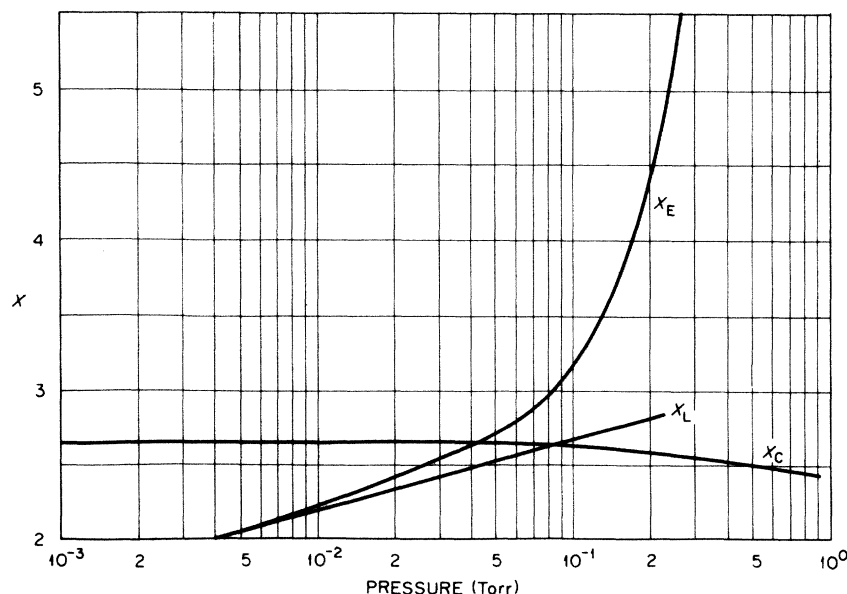At early times, most of the light emitted from

FIG. 7. Reduced frequency parameters vs pressure for the argon 1048-Å resonance line in the present geometry.

the cell comes from near the cylinder axis, and one can consider the transport problem in terms of resonance photons escaping from a slab geometry. At late times, however, the population of each volume element of the cylinder is such that the spatial profile remains constant (at least in the high- and low-pressure limits where a complete redistribution in frequency theory is appropriate); each volume element dV emits with the same frequency profile; the total number of excited states in each dV is decreasing exponentially. In general, the early-time and late-time escape rates will differ measurably. However, the ratio of $-d(\ln I)/dt$ at early and late times, with $I(t)$ defined by Eq. (51), is dependent on the parameter $y_0/2R$ and one can, in principle, choose this parameter so that at one pressure the ratio is unity.

To obtain an estimate of the appropriate value of $y_0/2R$, consider the low-pressure limits. We have shown that the assumption of complete redistribution in frequency gives nearly correct results. Only Doppler broadening is important, and the early-time value of $-d(\ln I)/dt$ can be equated to β_R as given in Eq. (30). The late-time decay rate β_L is determined by the fundamental mode of the eigenfunction expansion developed by Holstein.[5] We use the cylindrical geometry results of Payne and Cook[7] and find below 0.010 Torr,

$$\beta_R/\beta_L \approx 0.34(2R/y_0).$$ (52)

In this experiment $y_0/2R = 0.322$, so the early-time escape rate should only be about 5% faster than the late-time rate. One expects by interpolation that the escape rate at intermediate times will join these two smoothly, and one should be

able over an extended period of time to examine the escaping photons as an exponential decay with a single effective decay constant.

At pressures above 2 Torr, Doppler broadening plays no part in the transport process, and one calculates the ratio of early- to late-time escape rates β_E/β_L, using only the wing term of the profile,

$$\beta_E/\beta_L = 0.62(2R/y_0)^{1/2}.$$ (53)

Thus, at high pressures the ratio is again near

TABLE I. Early-time decay rate as a function of pressure.

Pressure (Torr)	Measured decay rate at early times (μsec^{-1})
9.35	0.377
5.25	0.358 [a]
5.18	0.363
1.94	0.361
1.07	0.354
0.86	0.339
0.57	0.340
0.50	0.344 [a]
0.41	0.330
0.184	0.293
0.135	0.319 [a]
0.093	0.283
0.069	0.316 [a]
0.042	0.310
0.0206	0.382 [a]
0.0147	0.468
0.0100	0.620 [a]
0.0015	5.4 [a]

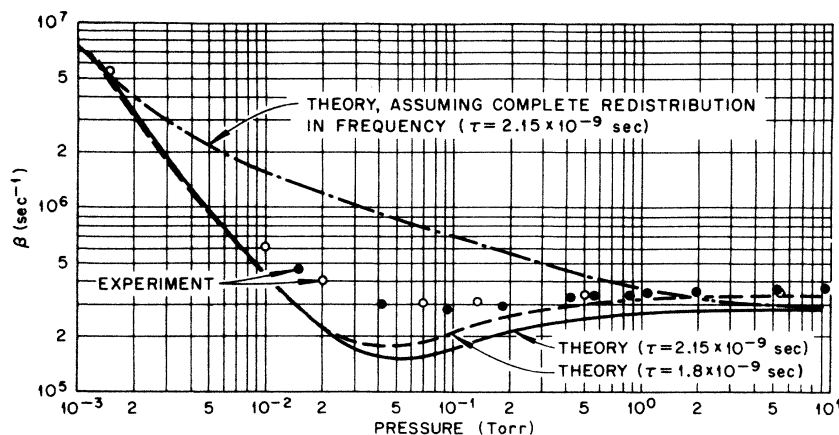[a] See text for comment on this later experiment.

FIG. 8. Experimental and theoretical early-time escape rates for argon 1048-Å resonance radiation. At pressures between 0.01 and 0.28 Torr the theory should give results that are two small owing to an approximation made in solving the transport theory.

unity with the early-time escape rate approximate-
ly 10% faster. The evaluation of $C(P, y_0, R)$ and
hence the computation of the time-integrated count
(intensity) will not be pursued further in this paper.

Typical data curves, plotting $I(t)\Delta t$ versus
time on a logarithmic scale, are shown in Fig. 5.
To compare the data with the theoretical calcula-
tions, the early-time slope was determined by a
least-squares fit giving additional weight to the
counts in earlier time channels. Experimental
and theoretical values of β are given in Table I
and in Fig. 8. The natural lifetime $\tau = 1/\gamma$ of the
$^1P_1$ argon state is somewhat uncertain. Two rea-
sonable values are 2.15×10^{-9} sec[21] and 1.8×10^{-9}
sec.[17] Curves representing both values are shown
in Fig. 8. A measurably different slope was ob-
served at late times at pressures above 0.5 Torr.
This slope is found to have a constant value of
0.32×10^6 sec^{-1}. Using the expression for β_L
implied from Eq. (52) (for the late-time escape
rate from cylindrical geometry[7]), this value is in
good agreement with the 1.8×10^{-9}-sec natural
lifetime. In addition, the results obtained by
applying the Holstein-Biberman equation at early
times with the complete redistribution assumption
is shown. [This is obtained from Eq. (48) with
P_c set equal to unity.] The errors on the slope
measurements are estimated to be less than
±3% except for the data point at 0.0015 Torr which
is ±20%.

The data points marked with an $\bigcirc$ in Fig. 8 and
indicated by footnote a in Table I were taken at a
later time and under different vacuum pumping
conditions than the rest of the data. In this later
set of experiments, an impurity was present which
would tend to increase the observed escape rate
of the resonance photons from the container. These
later data fall on a smooth curve which below 0.3
Torr lie approximately 0.03 μsec^{-1} above the data
determined in the earlier experiments where the
impurity was not present. At pressures above
0.3 Torr, the earlier and later experimental points
are the same within experimental error, suggesting
that in the process of flowing the argon gas, vis-
cous flow is sweeping out this impurity. At lower
pressures, Knudsen flow would not appreciably
effect the partial pressure of the impurity.

Several experimental and theoretical factors
can cause a difference between calculated and ob-
served escape rates. In general, all these factors
tend to cause the measured escape rate to be
faster than that determined from the theory. *Some
of these effects* [i.e., ones such as (4) below which
can be reduced by considering sufficiently early
times after the proton pulse], *however, are not
so critical here owing to the selected value of
$y_0/2R$ which tends to extend in time the early-time*
slope.

(a) The initial source function is not confined
rigorously to the cylinder axis as the diameter
of the proton beam is about 0.3 cm. In addition,
δ rays produced in the proton-argon collisions
may cause further spreading. Recombination of
ionized argon atoms could possibly serve as a
source function of $^1P_1$ excited atoms which would
be spread out in time and space, but experimental
data taken indicate that this is an unimportant
effect below 10 Torr.

(b) The initial $^1P_1$ excited states produced by the
proton beam, either directly or by cascade, will
have wings on the first emission even at lower
pressures. The emission spectrum will not be
quite a Voigt profile owing to the impulse given
the argon atoms by the protons. Those photons
emitted on the far wings in this first emission
should escape without further trapping. However,
no large initial burst of photons is observed in the
first few lifetimes (channel 1 of the analyzer).
The analysis of Sec. III shows that small deviations
initially present in the Doppler core of the profile
will not be retained for more than a few natural
lifetimes at low pressures. The emission profile
quickly approaches distribution which falls off a
bit more quickly than a Gaussian on the wings
where the effects of finite boundaries become
important.

(c) The value given for y_0 is obtained by mea-
suring the aperture diameter of the reaction cell.
Several factors may give a slightly smaller ef-
fective y_0: (i) the intrinsic lack of focus in the
vertical plane of the Seya-Namioka geometry and
(ii) the possibility of a slight misalignment of the
SEM detector with respect to the exit slit. With a
smaller y_0, the measured escape rate at early
times would appear faster.

(d) In the slab geometry treatment, those photons
emitted with $|x| < x_0$ are not allowed to contribute to
the transport process, but are immediately re-
absorbed at $y = 0$. Only those photons with $|x| > x_0$
can escape from the slab. Thus, except for the
choice of $y_0/2R$ so as to make late and early rates
of decay equal, we would obtain an underestimate
of escape rate from the slab at late-enough times.

(e) An appreciable error at intermediate pres-
sures arises when the conditions listed after Eq.
(36) are not met. In particular, at pressures less
than 0.3 Torr, "diffusion in frequency space"
can occur for photons emitted on the wing. This
tendency of photons emitted and absorbed many
successive times on the wings violates the strict
coherence required in Sec. V. Owing to the greater
number of photons emitted with frequency nearer
the core, this "diffusion" will carry the average
photon frequency further from the core with each

successive emission, hence increasing the actual escape rate. At pressures below 0.01 Torr, this effect is not important because the wings are not required for escape.

(f) The extension of the gas volume to infinity in evaluating Eq. (48) will introduce a small error, again causing one to underestimate the rate of escape.

(g) At low pressures there will be errors due to the assumption of isotropic emission in deriving Eq. (4). Further, the $\bar{R}(x', x)$ used in the theory is not by any means exact.

In carrying out the computations for the escape rates, two computer codes have been developed, one for evaluating β from Eq. (48) for an arbitrary gas and cell parameter (i.e., y_0) and one for evaluating $M(y, y')$ of Eq. (24).

APPENDIX

The function $U(x, \alpha)$ is related to the Kummer function.[22] However, since a tabulation of its properties does not seem to be readily available, we will list some of them here.

Relations involving $U(x, \alpha)$ can be determined from those involving $V(x, \alpha)$, where $\alpha > -1$,

$$V(x, \alpha) = \frac{2}{\pi} \int_0^\infty y^\alpha e^{-y^2} \cos(2xy) dy$$

$$= \Gamma[\tfrac{1}{2}(1 + \alpha)] \pi^{-1} M[\tfrac{1}{2}(1 + \alpha), \tfrac{1}{2}, -x^2]$$

$$= \Gamma[\tfrac{1}{2}(1 + \alpha)] \pi^{-1} e^{-x^2} M(-\tfrac{1}{2}\alpha, \tfrac{1}{2}, x^2). \quad \text{(A1)}$$

$M(a, b, Z)$ is Kummer's function.[22] Obviously,

$$U(x, \alpha) = -\frac{\partial V}{\partial \alpha}(x, \alpha). \quad \text{(A2)}$$

From (A1) we find

$$\frac{\partial^2 V}{\partial x^2} + 2x \frac{\partial V}{\partial x} + 2(1 + \alpha) V = 0. \quad \text{(A3)}$$

Thus,

$$\int e^{x^2} V(x, \alpha) dx = -\tfrac{1}{2}(1 + \alpha)^{-1} e^{x^2} \frac{\partial V(x, \alpha)}{\partial x} + C(\alpha)$$

$$\text{(A4)}$$

and

$$\int e^{x^2} \mathrm{erfc}(x) V(x, \alpha) dx = -\tfrac{1}{2}(1 + \alpha)^{-1} e^{x^2} \, \mathrm{erfc} \, \frac{\partial V(x, \alpha)}{\partial x}$$

$$- \pi^{-1/2}(1 + \alpha)^{-1} V(x, \alpha) + C'(\alpha). \quad \text{(A5)}$$

TABLE II. Tabulation of $U(x, 0)$.

x	$U(x, 0)$
0	0.5539
0.1	0.5540
0.2	0.5542
0.3	0.5541
0.4	0.5532
0.5	0.5510
0.6	0.5469
0.8	0.5311
1.0	0.5037
1.2	0.4461
1.4	0.4219
1.6	0.3760
1.8	0.3324
2.0	0.2936
2.1	0.2765
2.2	0.2608
2.3	0.2466
2.4	0.2337
2.5	0.2221
2.6	0.2115
2.7	0.2020
2.8	0.1933
2.9	0.1854
3.0	0.1782

Using (A2) we can evaluate $\int e^{x^2} U(x, \alpha) dx$ and $\int e^{x^2} \mathrm{erfc}(x) U(x, \alpha) dx$. The latter integrals are needed in showing that Eq. (22) satisfies Eq. (15) up to terms of order $\gamma^{-2} \partial^2 F(y, t)/\partial t^2$.

Of particular interest here is $U(x, 0)$. We find from (A2) and the properties of the Kummer function

$$U(x, 0) = \pi^{-1/2} e^{-x^2} \left(\tfrac{1}{2}\gamma + \ln 2 \right.$$

$$\left. + \sum_{n=0}^\infty \frac{(\sqrt{2} \, x)^{2n+2}}{2n + 2} \frac{1}{1 \cdot 3 \cdot 5 \cdots (2n + 1)} \right),$$

where γ is Euler's constant and equals $0.5772156649 \ldots$. Also,

$$\frac{\partial U}{\partial x}(x, 0) = -2x U(x, 0) + \mathrm{erf}(x).$$

At large x,

$$U(x, 0) = \tfrac{1}{2}x^{-1} + 1/(4x^3) + O(x^{-5})$$

$$- e^{-x^2} \pi^{-1/2} [\ln x - \tfrac{1}{4}x^{-2} + O(x^{-4})].$$

A tabulation of $U(x, 0)$ is given in Table II.

*Research sponsored by the U. S. AEC under contract with the Union Carbide Corporation.

†Graduate student from the University of Kentucky under appointment by Oak Ridge Associated Universities.

[1]M. W. Zemansky, Phys. Rev. 29, 513 (1927).

[2]M. W. Zemansky, Phys. Rev. 42, 843 (1932).

[3]A. C. G. Mitchell and M. W. Zemansky, *Resonance Radiation and Excited Atoms* (Macmillan, New York, 1934).

[4]H. W. Webb and H. A. Messenger, Phys. Rev. 33, 319 (1929).

[5]T. Holstein, Phys. Rev. 72, 1212 (1947); T. Holstein, Phys. Rev. 83, 1159 (1951).

[6]L. M. Biberman, Zh. Eksp. Teor. Fiz. 17, 584 (1949).

[7]M. G. Payne and J. D. Cook, Phys. Rev. A 2, 1238 (1970); C. van Trigt, Phys. Rev. 181, 97 (1969).

[8]C. E. Klots and V. E. Anderson, J. Chem. Phys. 56, 120 (1972).

[9]D. M. Bartell, G. S. Hurst, and E. B. Wagner, Phys. Rev. A 7, 1068 (1973).

[10]N. Thonnard and G. S. Hurst, Phys. Rev. A 5, 1110 (1972).

[11]W. Unno, Publ. Astron. Soc. Jap. 3, 158 (1952).

[12]W. Unno, Publ. Astron. Soc. Jap. 4, 100 (1952).

[13]D. L. Huber, Phys. Rev. 178, 93 (1969).

[14]H. Zanstra, Mon. Not. R. Astron. Soc. 101, 273 (1941).

[15]J. Jefferies and O. White, Astrophys. J. 132, 767 (1960).

[16]D. E. Osterbrock, Astrophys. J. 135, 195 (1962).

[17]P. R. Berman and W. E. Lamb, Phys. Rev. 187, 221 (1969).

[18]D. G. Hummer, Mon. Not. R. Astron. Soc. 125, 21 (1962); D. G. Hummer, Final Report, AFSWC Contract No. AF29(601)-6013 (unpublished).

[19]G. S. Hurst, T. E. Bortner, and T. D. Strickler, Phys. Rev. A 178, 4 (1969); T. E. Stewart, G. S. Hurst, T. E. Bortner, J. E. Parks, F. W. Martin, and H. L. Weidner, J. Opt. Soc. Am. 60, 1240 (1970).

[20]J. E. Talmage, Ph.D. thesis (University of Kentucky, 1973) (unpublished).

[21]G. M. Lawrence, Phys. Rev. 175, 40 (1968).

[22]*Handbook of Mathematical Functions*, edited by M. Abramowitz and I. A. Stegun (U. S. GPO, Washington, D.C., 1964).